Estuaries and Coasts (2012) 35:559–571
DOI 10.1007/s12237-011-9456-9

Nitrogen Sources and Rates of Phytoplankton Uptake in Different Regions of Hong Kong Waters in Summer

Jie Xu · Patricia M. Glibert · Hongbin Liu · Kedong Yin · Xiangcheng Yuan · Mianrun Chen · Paul J. Harrison

Received: 1 June 2011 / Revised: 19 September 2011 / Accepted: 18 October 2011 / Published online: 9 November 2011

Abstract Phytoplankton uptake rates of ammonium (NH_4^+), nitrate (NO_3^-), and urea were measured at various depths (light levels) in Hong Kong waters during the summer of 2008 using ^{15}N tracer techniques in order to determine which form of nitrogen (N) supported algal growth. Four regions were sampled, two differentially impacted by Pearl River discharge, one impacted by Hong Kong sewage discharge, and a site beyond these influences. Spatial differences in nutrient concentrations, ratios, and phytoplankton biomass were large. Dissolved nutrient ratios suggested phosphorus (P) limitation throughout the region, largely driven by high N loading from the Pearl River in summer. NH_4^+ and urea made up generally ≥50% of the total N taken up and the *f* ratio averaged 0.26. Even at the river-impacted site where concentrations of NO_3^- were >20 μM N, NH_4^+ comprised >60% of the total N uptake. Inhibition experiments demonstrated that NO_3^- uptake rates were reduced by 40% when NH_4^+ was >5 μM N. The relationship between the total specific uptake rates of N (sum of all measured substrates, *V*, per hour) and the chlorophyll *a*-specific rates (micromolars of N per microgram of Chl *a* per hour) varied spatially with phytoplankton biomass. Highest uptake rates and biomass were observed in southern waters, suggesting that P limitation and other factors (i.e., flushing rate) controlled production inshore and that the unincorporated N (mainly NO_3^-) was transported offshore. These results suggest that, at the beginning of summer, inshore algal blooms are fueled primarily by NH_4^+ and urea, rather than NO_3^-, from the Pearl River discharge. When NH_4^+ and urea are depleted, then NO_3^- is taken up and can increase the magnitude of the bloom.

Keywords Nitrate · Ammonium · Urea · N uptake · Pearl River discharge · Sewage effluent

J. Xu (✉) · H. Liu · X. Yuan · M. Chen · P. J. Harrison
Division of Environment, The Hong Kong University of Science and Technology,
Clear Water Bay,
Kowloon, Hong Kong SAR, People's Republic of China
e-mail: xujie@ust.hk

P. M. Glibert
Horn Point Laboratory, University of Maryland Center for Environmental Science,
P.O. Box 775, Cambridge, MD 21613, USA

H. Liu · M. Chen
Division of Life Science, The Hong Kong University of Science and Technology,
Clear Water Bay,
Kowloon, Hong Kong SAR, People's Republic of China

K. Yin
Environmental Futures Center, Griffith University,
Nathan Campus,
Brisbane, QLD 4111, Australia

Present Address:
X. Yuan
Key Laboratory of Tropical Marine Environmental Dynamics,
South China Sea Institute of Oceanology,
Chinese Academy of Sciences,
Guangzhou, China

Introduction

In recent years, anthropogenic nitrogen (N) loading has increased in many estuarine and coastal areas, and these external N inputs are due mainly to atmospheric deposition, land runoff, and local sewage effluent (Cloern 2001; Galloway and Cowling 2002; Galloway et al. 2002; Glibert et al. 2010). Enhanced riverine N inputs may affect N cycling in these estuarine ecosystems (e.g., Middelburg and Nieuwenhuize 2000; Howarth et al. 2002; Wassmann 2004). The changing composition of nutrients delivered to coastal waters is

beginning to be understood and quantified on both regional and global bases (e.g., Seitzinger et al. 2002, 2005; Harrison et al. 2005a, b; Boyer et al. 2006). It is now well recognized that both the total quantity of nutrients and their form impact the response of algae, ultimately affecting the extent to which new biomass is produced and by which species, as different species or species groups display preferences for specific nutrient regimes (Smayda 1990, 1997; Heisler et al. 2008).

The role of nutrient composition in affecting the growth, biomass, and species composition of algal blooms in coastal areas receiving high nutrient loads has been the focus of much attention. In particular, a great deal of attention has been focused on the interaction between NO_3^- and NH_4^+ uptake (Glibert 1982; Dortch 1990; Twomey et al. 2005; Lomas and Glibert 1999a, b, 2000; Dugdale et al. 2007). Diatoms often preferentially use NO_3^-, while flagellates often preferentially use more reduced forms of N (e.g., Lomas and Glibert 1999a, b, 2000; Glibert et al. 2006. The uptake of NO_3^- may be inhibited by NH_4^+, but this inhibition varies from no inhibition to complete inhibition, depending on the phytoplankton species, size, and their nutritional status and the environmental conditions (Dortch 1990; Lomas and Glibert 1999a, b; L'Helguen et al. 2008). In recent years, urea has also been recognized as an important nitrogenous nutrient that fuels algal growth and may regulate the uptake of other nitrogenous forms (Twomey et al. 2005; Glibert et al. 2006, 2008; Solomon et al. 2010).

Hong Kong waters are influenced year-round by local sewage discharge and, particularly in summer months, by Pearl River discharge. Hong Kong sewage treatment processes >2 million tonnes of sewage daily (Broom et al. 2003) and discharges approximately 49 tonnes of NH_4^+ day^{-1} after primary treatment (Choi et al. 2009). The Pearl River is the second largest river in China, next to the Yangtze River in terms of freshwater discharge, and in summer, its discharge reaches its annual maximum with high NO_3^- concentrations (~100 μM) with high molar N/P ratios (~100:1) (Yin et al. 2000, 2001). Hence, high loading of NH_4^+ from sewage and high NO_3^- from the Pearl River discharge enter Hong Kong waters during summer and provide regionally contrasting sites in terms of the dominant form of N (Xu et al. 2008, 2009). Freshwater input from the Pearl River not only contributes high N, but also contributes to water column stratification, which further favors phytoplankton growth. As a consequence, phytoplankton biomass reaches a seasonal maximum in summer and algal blooms (>10 μg chlorophyll *a* (Chl *a*) L^{-1}) can occur in the freshwater-influenced areas where diatoms commonly become dominant (Xu et al. 2009).

Little is known about the interactions among the uptake of different forms of N (NO_3^-, NH_4^+, and urea) and which form of nitrogenous nutrients fuel algal blooms during summer in Hong Kong waters, since previous studies on phytoplankton nutrition have focused mainly on phosphorus (P) uptake (Xu et al. 2008, 2009). This study, together with that of Yuan et al. (2011), represents the first efforts to determine factors regulating N utilization and the relative importance of NO_3^-, NH_4^+, and urea in Hong Kong waters during the development of summer algal blooms by measuring phytoplankton uptake rates of NO_3^-, NH_4^+, and urea using ^{15}N tracer techniques. Four regionally contrasting sites were examined, covering areas differentially affected by the Pearl River, Hong Kong sewage effluent, as well as one site beyond these influences.

Materials and Methods

Study Sites

Four stations (Fig. 1) were selected to represent different geographical regions and water quality zones: NM2 in western waters is affected by the Pearl River; VM5 in Victoria Harbour is affected by local sewage effluent; SM6 in southern waters represents the estuarine plume; and PM7 is in the eastern side of Hong Kong and not influenced directly by the river or sewage discharges. These are the same stations as sampled by the Hong Kong Environmental Protection Department's (EPD) monitoring program. Cruises were conducted at NM2 on July 2, at VM5 and SM6 on July 2 and 4, and at PM7 on July 3, 7, and 8, 2008. Water samples were collected at the surface (1 m), middle (4 m), and bottom (2 m above the sediment surface) at all stations. Vertical profiles of salinity and temperature were measured with a YSI 6600. Photosynthetically active radiation was measured with a Li-Cor underwater spherical quantum sensor (LI 193SA, USA); these data were used to estimate light levels for incubation. Rainwater was collected by putting a beaker for half an hour outside the laboratory at the Hong Kong University of Science and Technology in a rain event that occurred on July 13, 2008, to determine the nutrient input from this source.

Nutrients and Chlorophyll *a*

Nutrient samples were filtered through precombusted GF/F glass fiber filters and immediately frozen until analyzed. Inorganic nutrient concentrations were determined colorimetrically (Parsons et al. 1984) with a SKALAR autoanalyzer. Concentrations of NO_3^-+NO_2^- were analyzed by the Cu–Cd column reduction method and NH_4^+ with the indophenol blue color formation. Urea concentrations were measured with diacetyl monoxime thiosemicarbizade (Price and Harrison 1987). All N values are reported as micromolar N. Herein, total dissolved N (TDN) was defined as

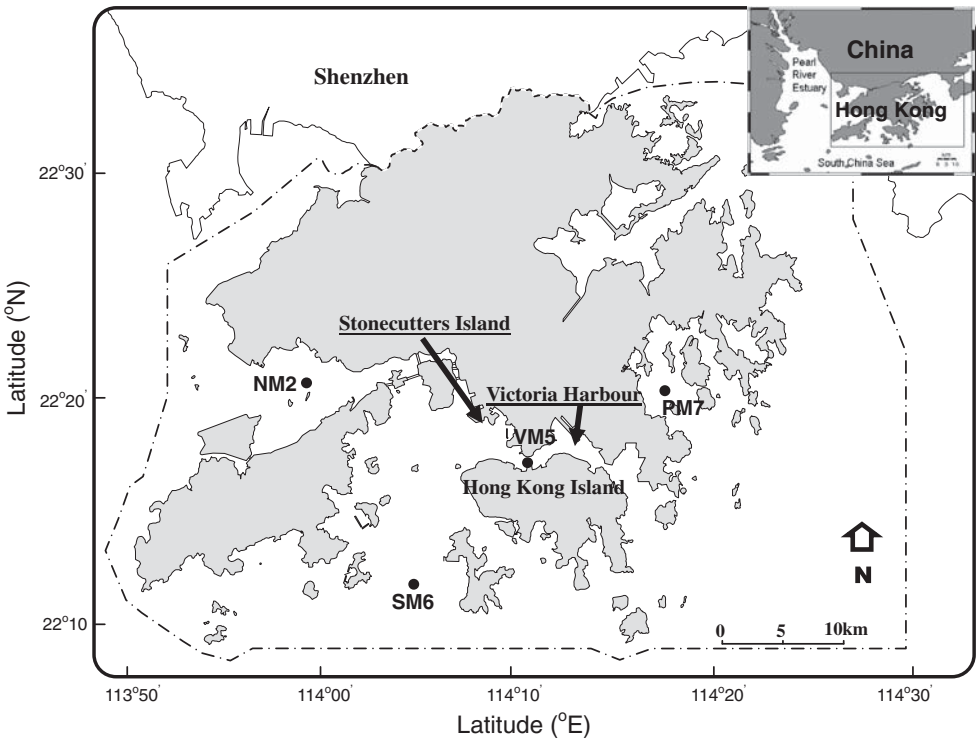

Fig. 1 Location of the sampling stations in Hong Kong waters. These four stations are the same as the EPD monitoring stations. The water depths for NM2, VM5, SM6, and PM7 are 11, 13, 15, and 17 m, respectively

$NO_3^-+NO_2^-+NH_4^+$+urea, recognizing that this designation is not typical since it includes urea but not other forms of organic nitrogen (for which there are no available data). Soluble orthophosphate (PO_4^{3-}) concentrations were measured using the ascorbic acid method, and silicate ($Si(OH)_4$) concentrations were analyzed using molybdate, oxalic acid, and a reducing reagent. Chl *a* was filtered onto Whatman GF/F glass fiber filters, extracted with 90% acetone, and analyzed using a fluorometer (Knap et al. 1996).

Particulate Biomass (PC, PN, and PP)

Samples for particulate carbon (PC) and particulate N (PN) were filtered through precombusted (460°C, 2 h) GF/F filters and later determined using a CHN analyzer. For particulate phosphate (PP) determinations, a filtered sample (precombusted GF/F filter) was placed in a 35-mL Teflon bottle, and then 10 mL of Milli-Q water and 1 mL of the oxidizing reagent (boric acid and potassium peroxodisulfate) were added. The bottle was autoclaved for at least 30 min. After cooling, PO_4^{3-} concentrations were determined with the SKALAR autoanalyzer (Grasshoff et al. 1999).

^{15}N Uptake

Water samples for ^{15}N uptake experiments were prefiltered through a 202-μm-mesh nylon screen. Ambient rates of N uptake were measured using ^{15}N-labeled NH_4^+, NO_3^-, and urea. ^{15}N substrates were added to the prescreened water samples at concentrations that were ~10% of ambient values. Single incubations were conducted at VM5 and SM6 and replicated incubations were conducted at NM2 and PM7 in polycarbonate bottles under five different light levels (100%, 50%, 30%, 10%, and 1% of ambient light) for 1 h. ^{15}N samples were incubated around noon, except for NM2 for which samples were incubated later in the afternoon. The surface samples were incubated at 100% and 50% light, the middle samples at 30% and 10% light, and the near-bottom samples at 1% light using neutral density screening in an on-deck incubator. The temperature of the incubator was maintained within ±2°C of in situ water temperature by running seawater. After incubation, samples were filtered onto precombusted GF/F filters and filters were frozen until mass spectrometry analysis using a Sercon mass spectrometer. PN-specific (V_{PN}, per hour) and absolute rates (ρ, micromolar per hour) were calculated according to Glibert and Capone (1993). Chl *a*-specific uptake rates (ρ_{chl}, micromolar N per microgram of Chl *a* per hour) were calculated by dividing ρ by the Chl *a* concentration.

The *f* ratio was calculated according to the following equation:

$$f\ \text{ratio} = \frac{\rho_{NO_3}}{\rho_{NO_3} + \rho_{NH_4} + \rho_{\text{urea}}} \quad (1)$$

where ρ_{NO_3}, ρ_{NH_4}, and ρ_{urea} are absolute uptake rates of NO_3^-, NH_4^+, and urea, respectively.

In addition to the experiments designed to measure ambient rates of uptake, a suite of experimental manipulations were conducted to measure the potential inhibition

of NO_3^- uptake by NH_4^+. These experiments were conducted at SM6 and VM5 on July 2, as well as PM7 on July 7 and 8, representing a range of ambient nutrient conditions. At each site, water was collected from three light levels (except for PM7 on July 8, which was only surface, 100% light) and prescreened as described above. The experimental manipulations involved the addition of unlabelled NH_4^+ at concentrations of 5, 10, and/or 20 μM N, and then samples were enriched with ^{15}N–NO_3^- and incubated and subsequently analyzed as described above. One station and treatment (PM7) was fully replicated and 25% of all experimental samples were replicated.

Statistical Analysis

Statistical analysis was performed using the SPSS software. A paired *t* test was conducted to determine the significant difference between V_{PN} and ρ_{chl} at all light levels for each station (α=0.05) and an analysis of variance was conducted on the experimental treatments.

Results

Salinity and Temperature

The water column was strongly stratified at all stations in summer. The surface salinity was lowest (~12) at NM2 due to the strong influence of the Pearl River discharge and the highest salinity (~25) occurred at PM7 where there was no input from the Pearl River discharge (Fig. 2). Surface salinity increased, temperature decreased by ~0.2°C, and stratification weakened at VM5 and SM6 on July 4 due to tidal mixing compared to July 2 (Fig. 2).

Dissolved Nutrients and Nutrient Ratios

Concentrations of all nutrients exhibited clear spatial variability, with the highest (up to 40 μM N NO_3^-, >1.2 μM P PO_4^{3-}, and >60 μM Si $Si(OH)_4$) at NM2, intermediate (generally 12–25 μM N NO_3^-, 0.2–1.0 μM P PO_4^{3-}, and 20–52 μM Si $Si(OH)_4$) at VM5 and SM6, and lowest (<2 μM N NO_3^-, <0.1 μM P PO_4^{3-} at the surface, and <25 μM Si $Si(OH)_4$) at PM7 (Fig. 3). NH_4^+ concentrations were up to 20 μM N at NM2, generally <6 μM N at the remaining stations, and were undetectable at PM7 and on July 2 at VM5 and July 4 at SM6. Urea concentrations were mostly <5 μM N and declined in concentration from station NM2 to VM5 and SM6, with the lowest at PM7 (Fig. 3).

The ratios of TDN/PO_4^{3-} were much greater than the Redfield ratio and averaged 42:1, 34:1, 53:1, and 50:1 at stations NM2, VM5, SM6, and PM7, respectively. Ratios of TDN/$Si(OH)_4$ were <1:1 and ratios of $Si(OH)_4$/PO_4^{3-} were >16:1 at all stations (Fig. 4).

Rainwater contained high N concentrations (15.1 μM N NO_3^-+NO_2^-, 7.8 μM N NH_4^+) and low PO_4^{3-} (0.24 μM P) and the DIN (=NO_3^-+NO_2^-+NH_4^+)/PO_4^{3-} ratio was 96:1. Urea was not measured in rainwater.

Particulate Carbon, Nitrogen, Phosphorus, and Chl *a*

Maximum particulate biomass occurred at SM6 on July 4. At the other stations, PC, PN, and PP were generally 30–60 μM C, 3–8 μM N, and 0.2–0.6 μM P, respectively (Fig. 5). PC/PN ratios fluctuated around 6.6:1 at the surface and middle layers of all stations, but at NM2, PC/PN ratios were ~9:1 (Fig. 6). PN/PP ratios were near 16:1 at NM2, VM5, and SM6, but were >30:1 at the surface at PM7. PC/PP ratios at the surface were near 106:1 at VM5 and SM6 and were >170:1 at NM2 and PM7 (Fig 6).

There was considerable spatial variation in Chl *a* concentrations. In the surface and middle layers, Chl *a* concentrations were low (mostly <4.5 μg L^{-1}) at NM2 and PM7 and relatively high (6–14 μg L^{-1}) at VM5 and SM6 (Fig. 7).

Uptake of Nitrogen (V_{PN}, ρ, and ρ_{chl})

The coefficients of variation in ^{15}N uptake rates calculated from replicated ^{15}N uptake samples were consistently <0.10 (not shown). There were clear spatial variations in V_{PN} and ρ with higher rates (up to 0.054 h^{-1} and 0.638 μM N h^{-1}, respectively) at SM6 and lower rates (maximum V_{PN} and ρ not exceeding 0.026 h^{-1} and 0.115 μM N h^{-1}, respectively) at other stations (Fig. 8). Maximum ρ_{chl} values at different light levels were 0.05–0.08 μM N (μg Chl *a*)$^{-1}h^{-1}$ at all stations, except for VM5 where ρ_{chl} values were comparatively low (<0.01 μM N (μg Chl *a*)$^{-1}h^{-1}$) (Fig. 8). The difference between V_{PN} and ρ_{chl} at various light levels was not significant (p>0.05) for SM6, but was significant (p<0.05) for NM2 and PM7.

Relative Uptake of Different N Forms

The relative importance of different N forms for samples from different irradiance levels was calculated using the average of two light levels (100% and 50%) for surface water samples and (30% and 10%) for middle water samples and was estimated from the single measurement in near-bottom water samples (1%). NH_4^+ dominated total N uptake (typically >50%, ranging from 6% to 82%) at most stations. NO_3^- was not the dominant form of N taken up, with one exception (SM6 on July 4) where NH_4^+ was undetectable and NO_3^- and urea

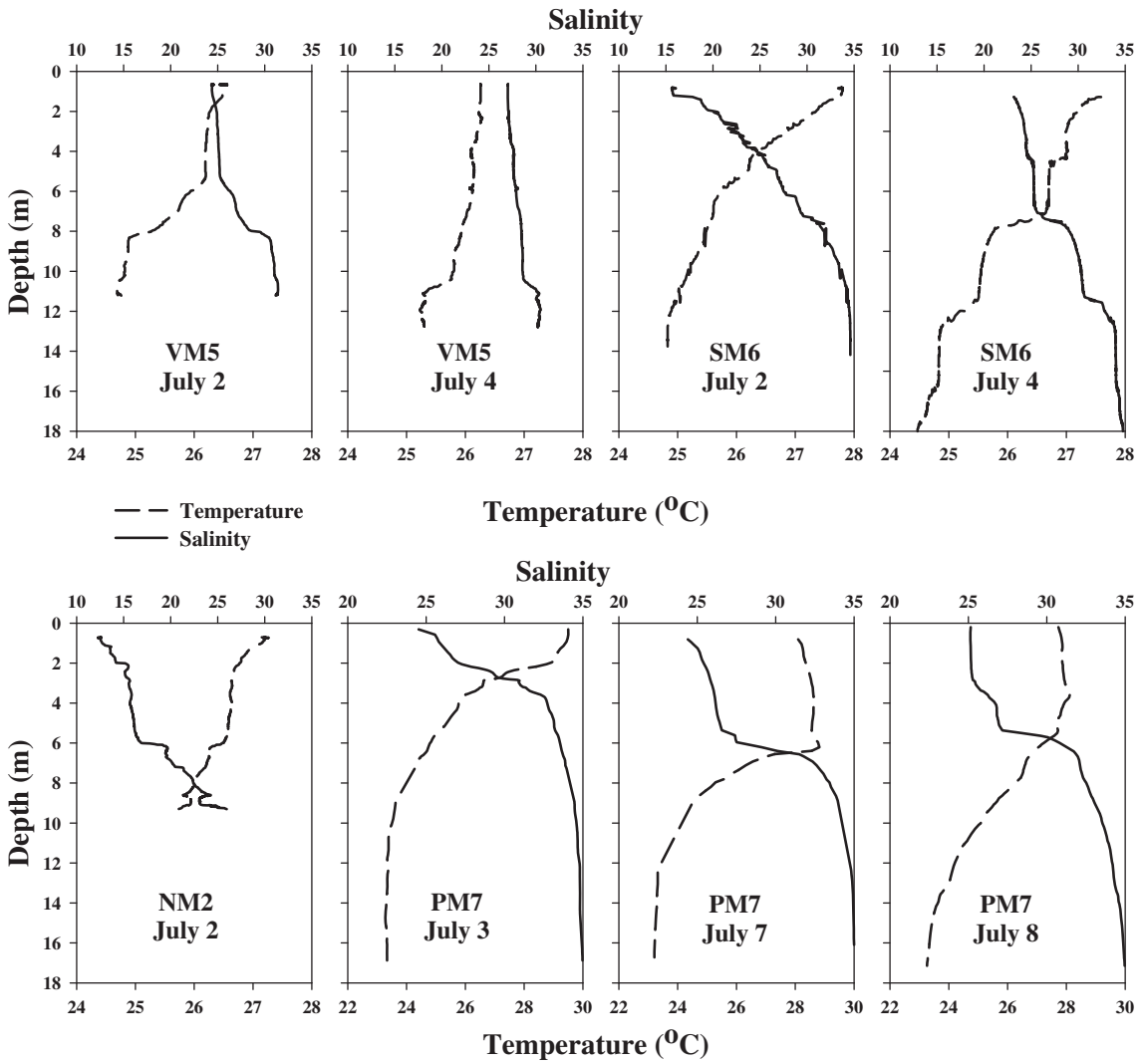

Fig. 2 The vertical distribution of salinity and temperature at the study sites (NM2, VM5, SM6, and PM7) in July 2008

dominated total uptake with 52% and 44%, respectively (Table 1). Urea was responsible for most of the total N uptake with 59% at VM5 on July 2 when NH_4^+ was undetectable (Table 1).

NO_3^- Inhibition by NH_4^+

Experimentally added NH_4^+ inhibited the ambient rate of NO_3^- uptake, on average, by ~40%, when all experiments and sites were combined, a significant ($p<0.05$) change relative to the unamended rates (Fig. 9). Although individual stations and/or treatments (e.g., stations SM6 and VM5, 30% and 1% irradiance levels, respectively; Fig. 9) were suggestive of increasing inhibition with increasing concentrations of NH_4^+, such a pattern was not significant when all results were combined. Thus, on average, an NH_4^+concentration of 5 μM N was sufficient to result in significant inhibition of NO_3^- uptake.

Discussion

Pearl River Discharge, Rainfall, Dissolved Nutrients, and Particulate Biomass

In summer, the Pearl River discharge invades western and southern waters of Hong Kong, lowers the surface salinity, and increases the NO_3^- concentration (Harrison et al. 2008). In contrast, at Port Shelter (PM7), on the eastern side of Hong Kong that is not influenced by the Pearl River, most of the N inputs come from rainfall and land runoff. As a result of the greatly reduced freshwater input, this station has a longer residence time compared to western waters that are more highly flushed (Lee et al. 2006).

A comparison of the nutrient ratios in the dissolved and particulate forms suggests that biomass at the different stations was differentially nutrient-limited. On one hand, with the exception of one sample from PM7, all stations

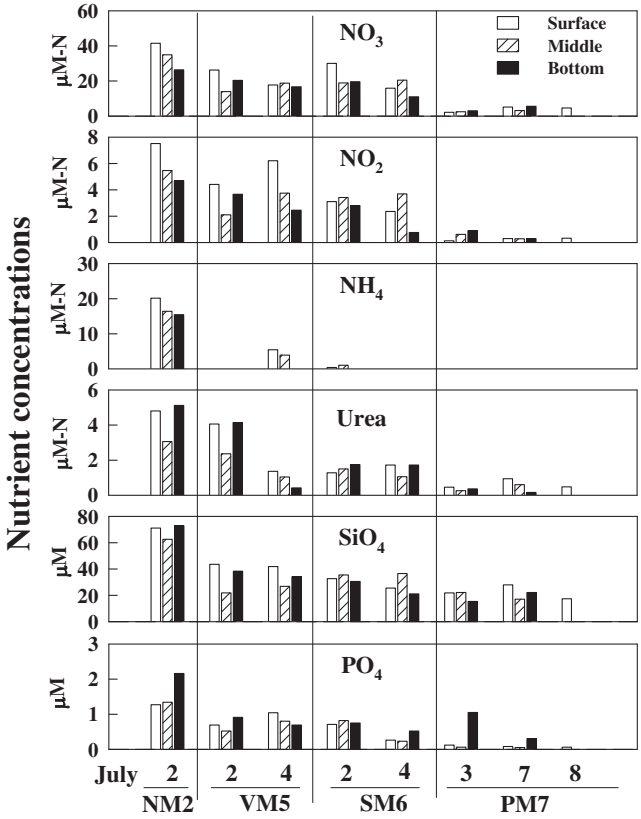

Fig. 3 Nutrient concentrations (NO_3, NO_2, NH_4, urea, PO_4, and SiO_4) at three depths (surface, middle, and bottom) at four stations in July 2008. Note that urea has two atoms N per mole

had ambient TDN/PO_4^{3-} ratios that were well above the Redfield ratio, ranging from 22 to 105 (Fig. 10). On the other hand, the molar N/P ratio of the particulate biomass, averaging 14:1 (Fig. 11), did not deviate from the Redfield ratio (Redfiled 1958) for the river and the Victoria Harbor station (NM2, VM5, and SM6). At these sites, even though the dissolved nutrient ratios were very high, the ambient PO_4^{3-} concentrations were also relatively high (0.23–2.2 μM). In contrast, at Port Shelter (PM7), elevated molar N/P ratios (20–39:1) of the particulate biomass at the surface were observed, along with high ambient dissolved N/P ratios (19–80:1) and low PO_4^{3-} concentrations (near or

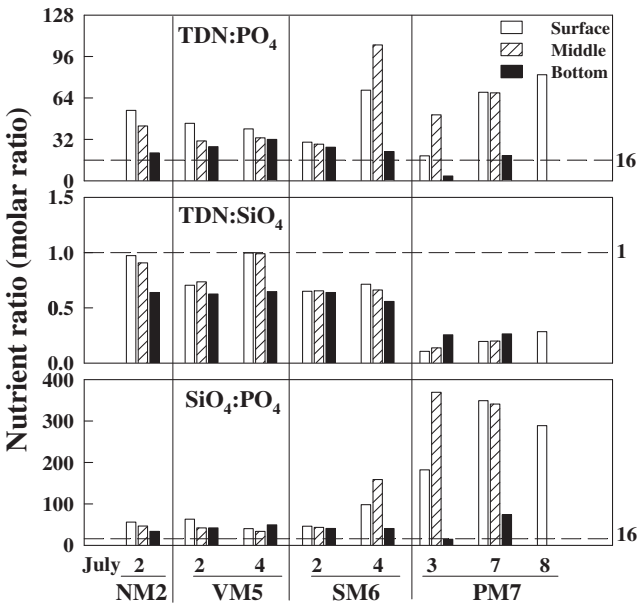

Fig. 4 Nutrient ratios depicted at three depths at four stations in July 2008. The *dashed lines* represent nutrient ratios of 16:1 (TDN/PO_4 or SiO_4/PO_4) and 1:1 (TDN/SiO_4). TDN=NH_4+NO_2+NO_3+urea

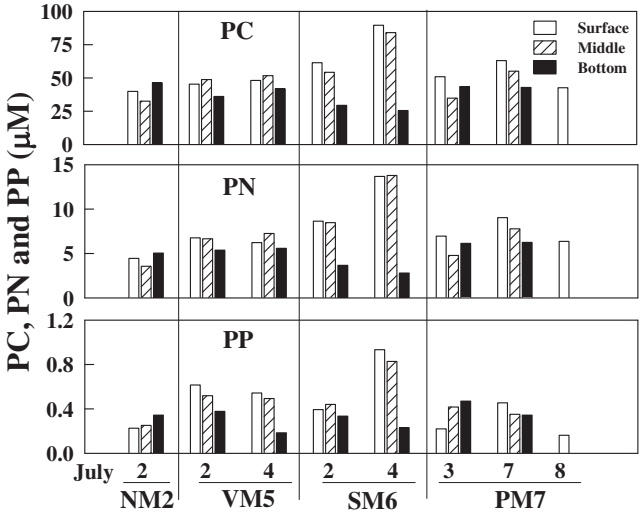

Fig. 5 Particulate carbon (*PC*), particulate nitrogen (*PN*), and particulate phosphorus (*PP*) at three depths (surface, middle, and bottom) at four stations in July 2008

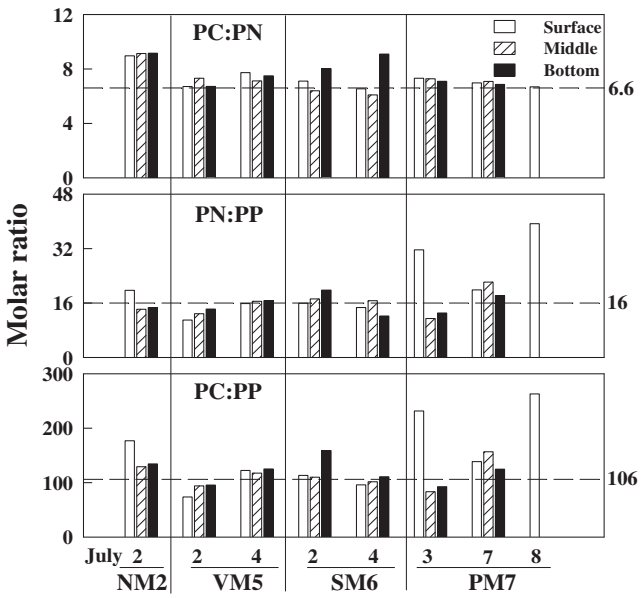

Fig. 6 PC/PN, PN/PP, and PC/PP ratios at three depths (surface, middle, and bottom) at four stations in July 2008. *PC* particulate organic carbon, *PN* particulate organic nitrogen, *PP* particulate organic phosphorus. The *dashed lines* denote the Redfield ratios of 6.6, 16, and 106 for PC/PN, PN/PP, and PC/PP, respectively

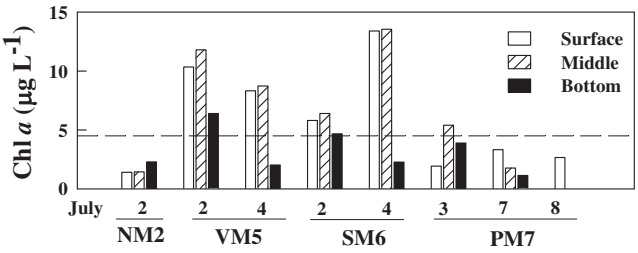

Fig. 7 Chl *a* concentrations at three depths (surface, middle, and bottom) at four stations in Hong Kong waters during July 2008. The *dashed line* denotes Chl *a* concentration of 4.5 μg L^{-1}, above which Chl *a*-containing algal biomass dominates the total PN tool

<0.1 μM P at the surface), suggesting that not only were ambient nutrients at P-limiting levels, but the phytoplankton biomass was also potentially P-limited. Moreover, the N/P ratios of both the particulate biomass and dissolved nutrients increased at PM7 between July 3 and 8, accompanied by a further reduction in the ambient PO_4^{3-} concentrations from 0.12 to 0.06 μM, suggesting that P limitation became more severe due to the continual rainfall which had a very high molar N/P (96:1) ratio during this study period (total rainfall was 11, 54, 39, and 51 mm on July 5, 6, 7, and 8, respectively). P limitation of phytoplankton biomass production and growth rate was previously documented at this site during July and inferred from nutrient enrichment bioassays and ^{33}P measurements (Xu et al. 2009). Phytoplankton at PM7 have previously been shown to be dominated by picocyanobacteria in terms of cell abundance (Chen et al. 2009), and picoplankton such as *Synechococcus* may be able to thrive under P-limiting conditions because they may be able to substitute normally P-requiring lipids with non-P-requiring lipids (Van Mooey et al. 2009).

Comparison of Nitrogen Uptake Rate (V_{PN}, ρ, and ρ_{chl})

It is difficult to accurately calculate phytoplankton-specific N uptake rates in situ as phytoplankton N content—exclusive of detritus and heterotrophs—cannot be directly measured. Currently, phytoplankton N concentrations are estimated primarily either by using Chl *a*/N ratios from laboratory cultures or by regression analysis of measured PN and Chl *a* concentrations (Dickson and Wheeler 1995). The regression analysis of particulate biomass and Chl *a* has been shown to be useful in estimating the average ratios of C/Chl *a* and N/Chl *a* for phytoplankton cells in the field (Dickson and Wheeler 1995; Chang et al. 2003). In Hong Kong waters, the average ratio of C/Chl *a* was estimated to be 42 g g^{-1} during summer (Fig. 11), similar to the mean value of 51 gg^{-1} previously reported for San Francisco Bay phytoplankton (Wienke and Cloern 1987). Phytoplankton C, estimated by multiplying the Chl *a* concentrations by the C/Chl *a* ratio of 42:1, accounted for 9–62% of the total PC pool (Table 2). Similar results (4–77%) were found for the English Channel by Holligan et al. (1984). Lowest proportions of phytoplankton C were found in the regions that were considered to be the most P-limited (NM2 and PM7).

The average N/Chl *a* ratio was estimated to be 0.66 μM N (μg Chl *a*)$^{-1}$ (Fig. 12), which fell within the previously reported range of 0.29–1.00 μM N (μg Chl *a*)$^{-1}$ for exponentially growing phytoplankton cells (Parsons et al. 1961; McCarthy and Nevins 1986). Based on this ratio, phytoplankton N was estimated to be 0.75–8.9 μM N and

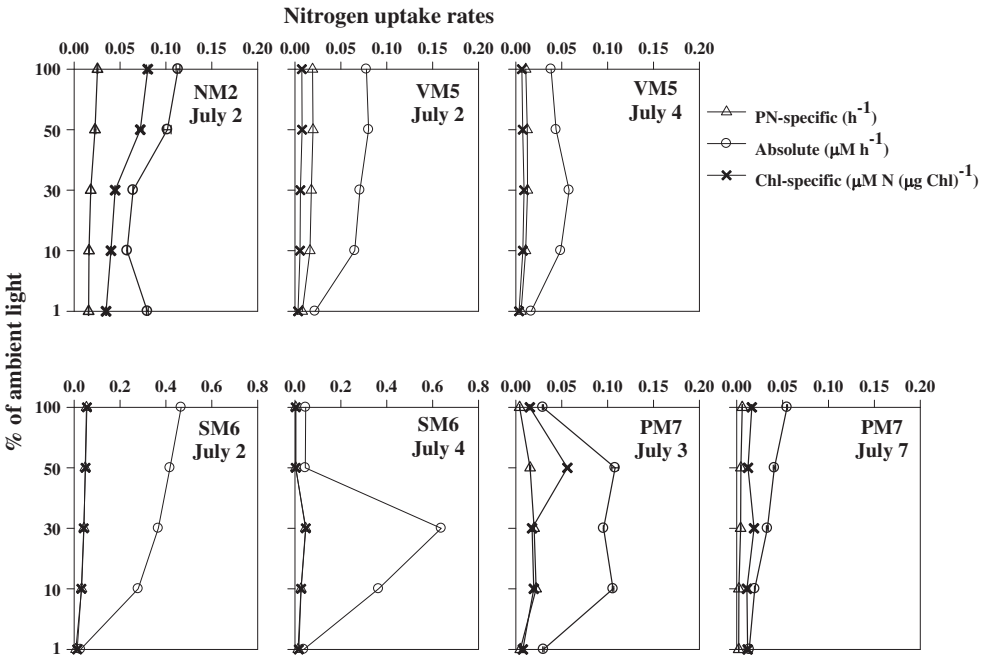

Fig. 8 PN-specific (per hour), absolute (micromolar per hour), and Chl *a*-specific uptake rates (micromolar N per microgram of Chl *a*) at five different light levels at NM2 on July 2, VM5 and SM6 on July 4, and PM7 on July 3, 2008. Note the different scales on the *x*-axis

Table 1 Fraction of uptake of different forms of N (±1 SD, n=3) at three depths at four stations

Station	Date	Depth	ρ_{urea}/ρ_{sum}	ρ_{NH_4}/ρ_{sum}	f ratio
NM2	July 2	Surface	0.06±0.01	0.64±0.01	0.30±0.01
		Middle	0.04±0.00	0.62±0.00	0.34±0.01
		Bottom	0.05	0.68	0.27
VM5	July 2	Surface	0.59±0.00	0.29±0.00	0.12±0.00
		Middle	0.61±0.02	0.31±0.01	0.08±0.01
		Bottom	0.51	0.29	0.21
	July 4	Surface	0.27±0.01	0.57±0.09	0.16±0.08
		Middle	0.27±0.01	0.56±0.03	0.17±0.02
		Bottom	0.16	0.34	0.50
SM6	July 2	Surface	0.12±0.01	0.82±0.00	0.06±0.01
		Middle	0.16±0.02	0.78±0.03	0.06±0.01
		Bottom	0.10	0.08	0.82
	July 4	Surface	0.44±0.04	0.04±0.01	0.52±0.05
		Middle	0.33±0.09	0.26±0.04	0.41±0.13
		Bottom	0.54	0.15	0.31
PM7	July 3	Surface	0.11±0.09	0.81±0.14	0.08±0.05
		Middle	0.42	0.15	0.43
		Bottom	NA	0.81	0.19
	July 7	Surface	0.16±0.00	0.66±0.00	0.18±0.00
		Middle	0.15±0.03	0.60±0.07	0.25±0.10
		Bottom	0.16	0.37	0.47

ρ_{urea}, ρ_{NH_4}, ρ_{NO_3}, and ρ_{sum} denote the absolute uptake rates of urea, NH_4, NO_3, and the total nitrogen (sum), respectively. The ρ_{urea}/ρ_{sum}, ρ_{NH_4}/ρ_{sum}, and f ratio denote the fraction of the uptake of urea, NH_4, and NO_3, respectively. The ρ_{urea}/ρ_{sum}, ρ_{NH_4}/ρ_{sum}, and f ratio were calculated from the average of two light levels (100% and 50%) for surface water samples and (30% and 10%) for middle water samples

NA data not available

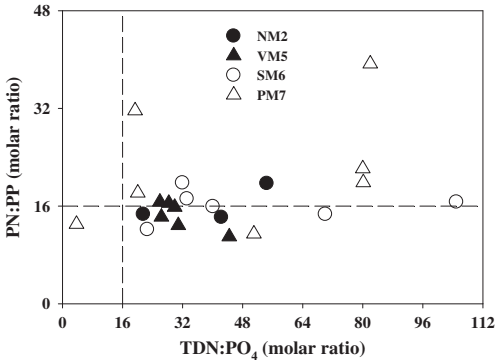

Fig. 10 Relationship between the molar ratio of the ambient total dissolved nitrogen pool (TDN/PO_4) and the molar ratio of the particulate biomass (PN/PP) for N/P. The *dashed line* denotes the Redfield stoichiometric proportions. The *open circles* denote the samples at river-impacted waters (NM2, VM5, and SM6). The *solid circles* denote the samples at PM7 (no river impact). TDN=NO_3+NO_2+NH_4+urea

accounted for 12–80% of the total PN pool (Table 2). As with C, the lowest proportions of phytoplankton N were found in the regions that were considered to be the most P-limited (NM2 and PM7). Similar results (9–76%) were reported for the Oregon–Washington shelf by Kokkinakis and Wheeler (1987). The relationship between Chl *a* concentrations and the percentage of phytoplankton N were best fitted to a rectangular hyperbola (Fig. 13). On this basis, Chl *a*-containing algal biomass should dominate the total PN pool (i.e., > 50%) when the phytoplankton biomass is >4.5 μg Chl *a* L^{-1}. Biomass values below this value, such as that observed at NM2 and PM7, may have been dominated by bacteria or zooplankton.

Comparisons of V_{PN} and ρ_{chl} showed that they varied spatially with phytoplankton biomass. V_{PN} and ρ_{chl} values were similar at all light levels at SM6 where Chl *a* concentrations were relatively high (generally >5 μg L^{-1}) and phytoplankton N comprised most of the total PN pool.

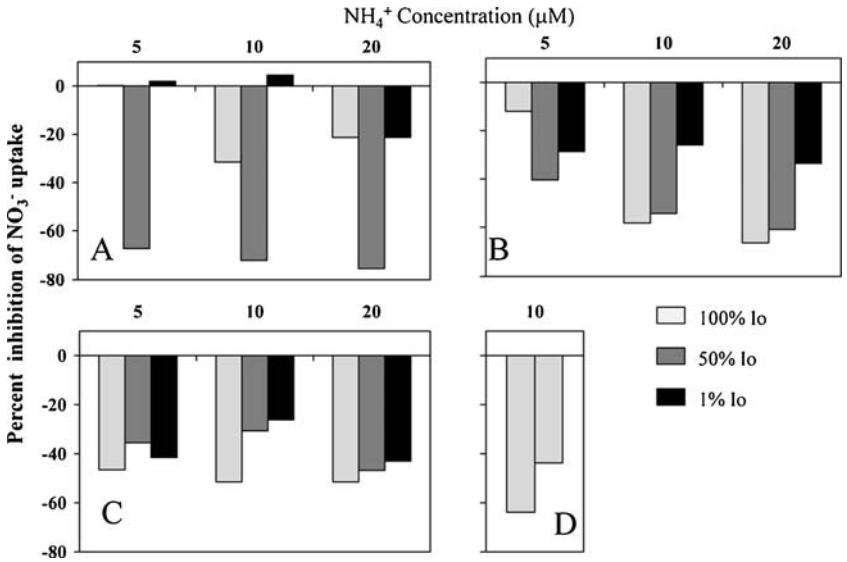

Fig. 9 Percent inhibition of NO_3^- uptake by NH_4^+ added at 5, 10, and 20 μM in experimental manipulations. **a** Station SM6 (southern waters), **b** station VM5 (Victoria Harbour), **c** station PM7 (eastern waters), and **d** surface water (100% light) at station PM7 replicated on the following day. Samples were collected and incubated at the light levels shown

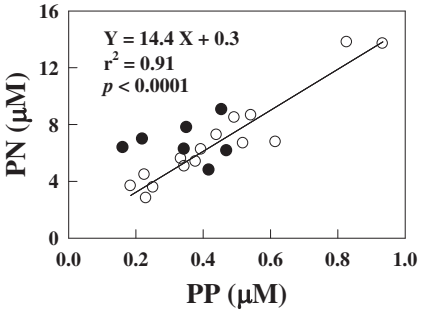

Fig. 11 A significant correlation between PN and PP for samples (*open circles*) in the river-impacted stations (NM2, VM5, and SM6) in July 2008. *PN* particulate organic nitrogen, *PP* particulate organic phosphorus. The samples (*solid circles*) at PM7 were excluded in the correlation of PN vs PP as P limitation might have occurred at PM7

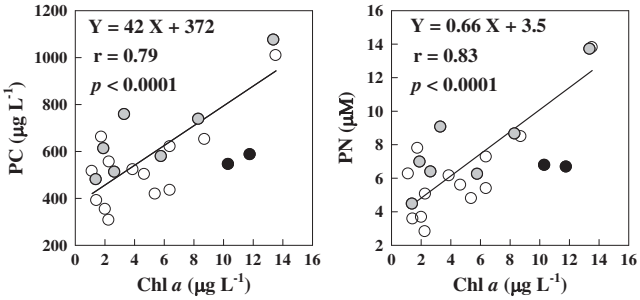

Fig. 12 A significant correlation between Chl *a* concentrations and PC and PN at three depths at four stations in Hong Kong waters during July 2008. The *gray solid circles* denote surface samples. The samples (*black solid circles*) at the surface and middle at VM5 on July 2 were excluded in the correlations of PN vs Chl *a* and PC vs Chl *a* as the PN and PC concentrations of these two samples were unexplainably low relative to Chl *a* concentrations

In contrast, V_{PN} was three to four times lower than ρ_{chl} at NM2 where Chl *a* concentrations were low (<2.5 μg L^{-1}) and phytoplankton N accounted for only ~30% of the total PN pool. It is speculated that bacteria might make a higher contribution to the total PN pool at NM2 than at other stations. This was supported by the previous report that attached bacteria made a higher contribution (~20%) to the total respiration in the western waters than that (~8%) in Victoria Harbour (Yuan et al. 2010). It is likely that total N uptake at NM2 was underestimated to a greater degree than at other stations due to higher recovery of the bacterial fraction on the filters (~20%; Yuan et al. 2010) and the late period in the day when these samples were incubated. The relatively high N uptake rate in near darkness (1% light level) may also be partially attributable to bacterial uptake.

Despite the large differences in V_{PN}, ρ, phytoplankton biomass, and nutrient concentrations among these stations, maximum ρ_{chl} rates at various light levels for each station varied in a relatively small range (0.05–0.08 μM N (μg Chl *a*)$^{-1}$h^{-1}), except for Victoria Harbour (VM5). In this study, Chl *a*-specific uptake rates were comparable to the observed

Table 2 Fraction of phytoplankton C and N in the total PC and PN pool

Stations	Date	Layer	Chl *a* μg L^{-1}	Phytoplankton N % of total PN	Phytoplankton C % of total PC
NM2	July 2	Surface	1.41	0.21	0.12
		Middle	1.44	0.27	0.16
		Bottom	2.29	0.30	0.17
VM5	July 2	Surface	10.3	NA	NA
		Middle	11.8	NA	NA
		Bottom	6.4	0.80	0.62
	July 4	Surface	5.81	0.62	0.42
		Middle	5.40	0.59	0.43
		Bottom	4.67	0.56	0.39
SM6	July 2	Surface	8.32	0.65	0.47
		Middle	8.73	0.69	0.56
		Bottom	2.03	0.37	0.24
	July 4	Surface	13.4	0.66	0.52
		Middle	13.5	0.66	0.56
		Bottom	2.27	0.54	0.31
PM7	July 3	Surface	1.93	0.19	0.13
		Middle	5.40	0.76	0.54
		Bottom	3.89	0.42	0.31
	July 7	Surface	3.33	0.25	0.18
		Middle	1.77	0.15	0.11
		Bottom	1.14	0.12	0.09
	July 8	Surface	2.66	0.28	0.22

Phytoplankton C and N were calculated using a C/Chl *a* ratio of 42 $gg^{-1}$and N/Chl *a* ratio of 0.66 μmol N (μg Chl)$^{-1}$

NA data not available

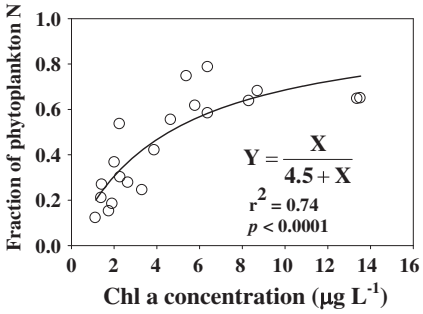

Fig. 13 Fraction of phytoplankton N in the total PN pool as a function of Chl *a* concentration for Hong Kong waters in summer 2008. The *line* was fit to a rectangular hyperbola. Data are from Table 2

values in the Oregon upwelling zone with high NO_3^- concentration in summer (Dickson and Wheeler 1995), in the western English Channel during spring and summer (L'Helguen et al. 1996), and the Ria de Ferrol in Spain during summer (Bode et al. 2005). These results indicated that the spatial changes in PN-specific uptake rates were primarily influenced by phytoplankton biomass and N concentrations, rather than phytoplankton-specific activity.

Regionally, the stations sampled ranged from the western site, NM2, which had low Chl *a*, low percent N and C in biomass, and low rates of uptake, but high ambient concentrations, to more productive and phytoplankton-dominated stations at VM5 and SM6. Low Chl *a*, low percent N and C in biomass, and low ambient nutrient concentrations were also characteristic of the eastern region, PM7. PN-specific and absolute uptake rates at SM6 were twofold and threefold higher than at stations NM2 and PM7. There are several reasons why the western-most site, NM2, may not be productive despite the high nutrient concentrations. High flushing rates (Ho et al. 2010), as well as high rates of grazing by mesozooplankton (which were excluded from our incubations) (Chen et al. 2009), may have held phytoplankton biomass at low levels. As suggested below, NH_4^+ may also have been at inhibitory concentrations for NO_3^- uptake at this site.

In contrast, higher phytoplankton biomass was observed at VM5 and SM6 and concentrations of NH_4^+ were unexpectedly low. This site is generally considered to be impacted by sewage effluent NH_4^+, but there was no significant accumulation of this nutrient at this site at the time of our sampling. Choi et al. (2009), using modeled distribution of the nutrient plume, suggest that, during the wet season, the plume of N effluent is depth-restricted between 6.5 and 9.5 m for >85% of the time. In winter, when N uptake is low, NH_4^+ concentrations are 15–20 μM at VM5 (Xu et al. 2008, 2009), indicating that the lower NH_4^+ concentrations in summer are, in addition, likely due to phytoplankton and bacterial uptake and some oxidation of NH_4 to NO_3^- when surface water temperatures reach 28–30°C, as well as dilution by freshwater (i.e., rainfall and runoff) (Xu et al. 2010). SM6 in southern waters is ~10 km from the discharge site and NH_4^+ is generally greatly diluted before it reaches this site, in addition to biological uptake. At Port Shelter (PM7), in addition to nutrient limitation, microzooplankton grazing may be one of the factors that were responsible for low phytoplankton biomass (Chen et al. 2009).

Interactions Among NO_3^-, NH_4^+, and Urea Uptake

The relative importance of primary production from allochthonous NO_3^- is commonly measured by the *f* ratio, the ratio of NO_3^- uptake to the uptake of all nitrogenous sources (Eppley and Peterson 1979). However, new production estimated from ^{15}N uptake measurements may be underestimated in coastal waters that are influenced by NH_4^+ and urea from sewage, rainfall, and land runoff (all new or allochthonous forms of N; Eppley and Peterson 1979). Thus, the *f* ratio herein does not actually reflect the relative contribution of new production to primary production, but rather identifies the relative importance of primary production based on NO_3^- from the Pearl River discharge relative to NH_4^+ and urea from other sources, both natural and anthropogenic.

In Hong Kong waters, some combination of a preference for NH_4^+ and an inhibition of NO_3^- uptake by NH_4^+ and urea were clearly evident. When NH_4^+ was high, NH_4^+ generally dominated the total N uptake rate (52–65%). When NH_4^+ was depleted, urea became a dominant component of the N uptake. When Chl *a* does accumulate in Victoria Harbour (VM5) and southern waters (SM6), the initial development of summer algal blooms are seemingly dependent primarily on NH_4^+ and urea, rather than NO_3^- from the Pearl River discharge. Our results agree with Yuan et al. (2011) who found that NH_4^+ and amino acid uptake potentially accounted for an important fraction of the total N uptake for the 0.7- to 8-μm-sized phytoplankton at the same stations as used in our study.

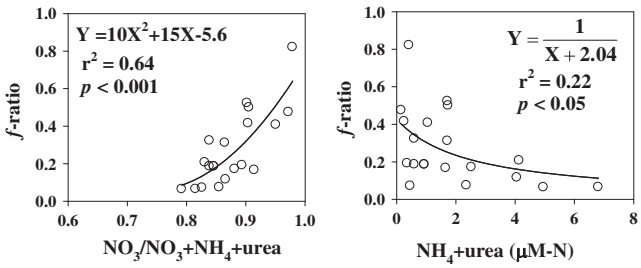

Fig. 14 A significant correlation between *f* ratio and the ambient NO_3/NO_3+NH_4+urea ratio (**a**) and NH_4+urea concentrations (**b**) at three depths at three stations (VM5, SM6, and PM7). Data are from Table 1

Even when NH_4^++urea concentrations declined to 0.2 μM, the *f* ratio (~0.4) suggested a preference for the reduced form of N. Furthermore, a significant correlation was observed between the *f* ratio and NH_4^++urea concentrations (Fig. 14). In addition, previous nutrient depletion bioassays conducted on a seasonal basis at the same four stations as this study showed that the highest assimilation of NO_3^- always occurs after NH_4^+ depletion (Xu 2007). Collectively, the nutrient depletion bioassays, the experimental inhibition experiments, and the *f* ratio analyses suggested that both NH_4^+ and urea were competitive inhibitors of NO_3^- uptake and the degree of inhibition depended on NH_4^+ and urea concentrations.

The inhibition of NO_3^- uptake by NH_4^+ and urea has been widely reported in field work and laboratory cultures (e.g., Glibert 1982; Dortch 1990; Lipschultz 1995; Dugdale et al. 2007). More specifically, Bates (1976) and Lund (1987) showed that NO_3^- uptake rates by *Skeletonema costatum* were inhibited 60% by 13 and 10 μM NH_4^+ additions, while Dortch and Conway (1984) found that, in N-sufficient cultures of *S. costatum*, NO_3^- uptake rates were inhibited 6% by 5 to 20 μM NH_4^+. For *Thalassiosira pseudonana*, on the other hand, similar NO_3^- uptake rates (no inhibition) was observed with daily pulses of 2 μM NH_4^+ (Berges et al. 1995), but rates by the same species were found to be completely inhibited by sustained NH_4^+ concentrations of 2 μM (Dortch et al. 1991). Lomas and Glibert (1999a, b) observed that NO_3^- uptake was less inhibited by NH_4^+ in diatoms than in dinoflagellates, but their findings, along with those of Bates (1976), Dortch and Conway (1984), and Dortch et al. (1991), suggest that the degree of inhibition is species-specific and a function of the preconditioning N source, degree of N limitation, growth rate, temperature, and light. Lomas and Glibert (1999a, b) concluded that high light tends to lessen the degree of NH_4^+ inhibition, a pattern also observed here (Fig. 9), but not statistically substantiated due to sample size. In addition, several studies have shown that some phytoplankton species grown on NH_4^+ or urea may have higher growth rates than on NO_3^- (Wood and Flynn 1995; Herndon and Cochlan 2007; Suksomjit et al. 2009; Solomon et al. 2010). Hence, it is speculated that summer algal blooms are fueled primarily by NH_4^+ and urea in the early stage of bloom development in Hong Kong waters, rather than NO_3^- from the Pearl River discharge. However, when NH_4^+ and urea are depleted, NO_3^- is then taken up and can increase the magnitude of the bloom (amount of Chl *a* produced). The Pearl River discharge likely triggers summer algal blooms by stratifying the water column in western and southern waters which favors the phytoplankton growth and accumulation of the phytoplankton cells (Ho et al. 2010).

Before the sewage treatment and subsequent nutrient reduction measures that were implemented in 2001 in Hong Kong, the maximum monthly average Chl *a* concentration in July in Victoria Harbour was 14 μg L^{-1} and the ambient monthly average NH_4^+ concentration was 6.6 μM N during 1986–2001 (Xu et al. 2008). These NH_4^+ concentrations were high enough to significantly inhibit NO_3^- uptake. A mass balance suggests that a Chl *a* concentration of ~14 μg L^{-1} should be produced by the ambient NH_4^+. If the remaining NH_4^+ concentration of 6.6 μM were converted to phytoplankton biomass, based on the N/Chl *a* ratio of 0.66 μM N (μg Chl *a*)$^{-1}$, the total phytoplankton biomass that could be produced would be 24 μg Chl *a* L^{-1}. This value was surprisingly consistent with the value of 25 μg Chl *a* L^{-1}, the amount of phytoplankton biomass that could be produced when NH_4 at the surface was utilized by phytoplankton, obtained from the regression of NH_4^+ concentration vs Chl *a* (Xu et al. 2008). In our study, since the sum of NH_4^++urea concentrations was always >1 μM N in sewage- or river-influenced waters, the estimated Chl *a* concentration that the NH_4^++urea sources could produce would be ~16 μg L^{-1} in Victoria Harbour in July, remarkably comparable to the observed maximum monthly average value. This result suggested that the phytoplankton standing stock in Victoria Harbour was mainly supported by NH_4^+, not NO_3^-, after nutrient reduction measures initiated in 2001.

A significant correlation between the *f* ratio and the $NO_3^-/(NO_3^-+NH_4^+$+urea) ratio in Hong Kong waters, except for NM2 (Fig. 13), suggested that the *f* ratio varied with the ambient nutrient pools, which supports the suggestion of NH_4^+ inhibition of NO_3^- and a preference for NH_4^+. This relationship has also been described for many other coastal areas (McCarthy et al. 1977; Harrison et al. 1987; Dugdale et al. 2007). We speculate that this inhibition would be partially overcome by increasing the portion of NO_3^- in the total dissolved N pool.

Station NM2 had an *f* ratio of ~0.3 that was higher than expected, since NH_4^+ concentrations were up to 20 μM N. While this site had very low Chl *a* values overall, the phytoplankton community was dominated by the diatom *S. costatum* (Chen et al. 2009; Xu et al. 2009). The findings here, where Chl *a*, phytoplankton C and N, and uptake rates were low at NM2, but higher at SM6, suggest that the N is transported further offshore where it may contribute to blooms when phytoplankton growth rate exceeds the flushing rate, with decreasing flushing rate along the offshore direction. While NH_4^+ and urea may contribute to Chl *a* inshore and nonpoint sources of N may contribute to picoplankton production along the eastern coast, the Pearl River discharge with high NO_3^- concentrations may have a greater influence offshore. The change in Chl *a* from July 2 to 4 at SM6 indicates the potential for production to be high in this region. The implications of these findings are that, while physical processes and P limitation are

potentially important controls on phytoplankton production and biomass inshore, N quality and quantity also have important controls on phytoplankton biomass and production both inshore and offshore.

Acknowledgements This research was supported by the University Grants Council of Hong Kong AoE project (AoE/P-04/04-4-II). This is a contribution of the GEOHAB Core Research Project on HABs in Eutrophic Systems. This is contribution number 4548 from the University of Maryland Center for Environmental Science.

References

Bates, S.S. 1976. Effects of light and ammonium on nitrate uptake by two species of estuarine phytoplankton. *Limnology and Oceanography* 21: 212–218.

Berges, J.A., W.P. Cochlan, and P.J. Harrison. 1995. Laboratory and field responses of algal nitrate reductase to diel periodicity in irradiance, nitrate exhaustion, and the presence of ammonium. *Marine Ecology Progress Series* 124: 259–269.

Bode, A., N. González, C. Rodríguez, M. Varela, and M.M. Varela. 2005. Seasonal variability of plankton blooms in the Rio de Ferrol (NW Spain): I. Nutrient concentrations and nitrogen uptake rates. *Estuarine Coastal and Shelf Science* 63: 269–284.

Boyer, E.W., R.W. Howarth, J.N. Galloway, F.J. Dentener, P.A. Green, and C.J. Vorosmarty. 2006. Riverine nitrogen export from the continents to the coasts. *Global Biogeochem Cycles* 20: GB1S91. doi:10.1029/2005GB002537.

Broom, M., G. Chiu, and A. Lee. 2003. Long-term water quality trends in Hong Kong. In *Perspectives on marine environment change in Hong Kong and Southern China, 1977–2001*, ed. B. Morton, 534. Hong Kong: Hong Kong University Press.

Chang, J., F.K. Shiah, G.C. Gong, and K.P. Chiang. 2003. Cross-shelf variation in carbon-to-chlorophyll *a* ratios in the East China Sea, summer 1998. *Deep-Sea Research Part II* 50: 1237–1247.

Chen, B., H. Liu, M.B. Landry, M. Chen, J. Sun, L. Shek, X. Chen, and P.J. Harrison. 2009. Estuarine nutrient loading affects phytoplankton growth and microzooplankton grazing at two contrasting sites in Hong Kong coastal waters. *Marine Ecology Progress Series* 379: 77–90.

Choi, K.W., J.H.W. Lee, K.W.H. Kwok, and K.M.Y. Leung. 2009. Integrated stochastic environmental risk assessment of the harbor area treatment scheme (HATS) in Hong Kong. *Environmental Science and Technology* 43: 3705–3711.

Cloern, J.E. 2001. Our evolving conceptual model of the coastal eutrophication problem. *Marine Ecology Progress Series* 210: 223–253.

Dickson, M.L., and P.A. Wheeler. 1995. Nitrate uptake rates in a coastal upwelling regimes: A comparison of PN-specific, absolute, and Chl *a*-specific rates. *Limnology and Oceanography* 40: 533–543.

Dortch, Q. 1990. The interaction between ammonium and nitrate uptake in phytoplankton. *Marine Ecology Progress Series* 61: 183–201.

Dortch, Q., and H.L. Conway. 1984. Interactions between nitrate and ammonium uptake: Variation with growth rate, nitrogen source and species. *Marine Bioloby* 79: 151–164.

Dortch, Q., P.A. Thompson, and P.J. Harrison. 1991. Short-term interaction between nitrate and ammonium uptake in *Thalassiosira pseudonana*: Effect of preconditioning nitrogen source and growth rate. *Marine Biology* 110: 183–193.

Dugdale, R.C., F.P. Wilkerson, V.E. Hogue, and A. Marchi. 2007. The role of ammonium and nitrate in spring bloom development in San Francisco Bay. *Estuarine, Coastal and Shelf Science* 73: 17–29.

Eppley, R.W., and B.J. Peterson. 1979. Particulate organic matter flux and planktonic new production in the deep ocean. *Nature* 282: 677–680.

Galloway, J.N., and E.B. Cowling. 2002. Nitrogen and the world: 200 years of change. *Ambio* 31: 64–71.

Galloway, J.N., E.B. Cowling, S.P. Seitzinger, and R.H. Socolow. 2002. Reactive nitrogen: Too much of a good thing. *Ambio* 31: 60–63.

Glibert, P.M. 1982. Regional studies of daily, seasonal and size fraction in ammonium remineralization. *Marine Biology* 70: 209–222.

Glibert, P.M., and D.G. Capone. 1993. Mineralization and assimilation in aquatic, sediment, and wetland systems. In *Nitrogen isotope techniques*, ed. R. Knowles and T.H. Blackburn, 243–271. San Diego: Academic.

Glibert, P.M., J. Harrison, C. Heil, and S. Seitzinger. 2006. Escalating worldwide use of urea—A global change contributing to coastal eutrophication. *Biogeochemistry* 77: 441–463.

Glibert, P.M., R. Azanza, M. Burford, K. Furuya, et al. 2008. Ocean urea fertilization for carbon credits poses high ecological risks. *Marine Pollution Bulletin* 56: 1049–1056.

Glibert, P.M., J.I. Allen, L. Bouwman, C. Brown, K.J. Flynn, A. Lewitus, and C. Madden. 2010. Modeling of HABs and eutrophication: Status, advances, challenges. *Journal of Marine Systems* 83: 262–275.

Grasshoff, K.M., K. Kremling, and M. Ehrhardt. 1999. *Methods of seawater analysis*. New York: Wiley-VCH.

Harrison, W.G., T. Platt, and R. Lewis. 1987. *f*-ratio and its relationship to ambient nitrate concentration in coastal waters. *Journal of Plankton Research* 9: 249–253.

Harrison, J.H., N.F. Caraco, and S.P. Seitzinger. 2005a. Global patterns and sources of dissolved organic matter export to the coastal zone: Results from a spatially explicit, global model. *Global Biogeochem Cycles* 19: GBS406.

Harrison, J.H., S.P. Seitzinger, N. Caraco, A.F. Bouwman, A. Beusen, and C. Vörösmarty. 2005b. Dissolved inorganic phosphorous export to the coastal zone: Results from a new, spatially explicit, global model (NEWS-SRP). *Global Biogeochemical Cycles* 19 (4): GB4S03.

Harrison, P.J., K.D. Yin, J.H.W. Lee, J.P. Gan, and H.B. Liu. 2008. Physical–biological coupling in the Pearl River Estuary. *Continental Shelf Research* 28: 1405–1415.

Heisler, J., P. Glibert, J. Burkholder, D. Anderson, W. Cochlan, W. Dennison, Q. Dortch, C. Gobler, C. Heil, E. Humphries, A. Lewitus, R. Magnien, H. Marshall, K. Sellner, D. Stockwell, D. Stoecker, and M. Suddleson. 2008. Eutrophication and harmful algal blooms: A scientific consensus. *Harmful Algae* 8: 3–13.

Herndon, J., and W.P. Cochlan. 2007. Nitrogen utilization by the raphidophyte *Heterosigma akashiwo*: Growth and uptake kinetics in laboratory cultures. *Harmful Algae* 6: 260–270.

Ho, A.Y.T., J. Xu, K. Yin, Y. Jiang, X. Yuan, L. He, D.M. Anderson, J.H.W. Lee, and P.J. Harrison. 2010. Phytoplankton biomass and production in subtropical Hong Kong waters: Influence of Pearl River outflow. *Estuaries and Coasts* 33: 170–181.

Holligan, P.N., R.P. Harris, R.C. Newell, D.S. Harbour, R.N. Head, E. A.S. Linley, M.I. Lucas, P.R.G. Tranter, and C.M. Weekley. 1984. Vertical distribution and partitioning of organic carbon in mixed, frontal and stratified waters of the English Channel. *Marine Ecology Progress Series* 14: 111–127.

Howarth, R.W., A. Sharpley, and D. Walker. 2002. Sources of nutrient pollution to coastal water in the United States: Implications for achieving coastal water quality goals. *Estuaries* 25: 656–676.

Knap, A., A. Michaels, A. Close, H. Ducklow, and A. Dickson. 1996. [eds]. Protocols for the Joint Global Ocean Flux Study (JGOFS) Core Measurements. JGOFS report No 19, vi+170 pp. Reprint of the IOC Manual and Guides No. 29, UNESCO 1994.

Kokkinakis, S.A., and P.A. Wheeler. 1987. Nitrogen uptake and phytoplankton growth in coastal upwelling regions. *Limnology and Oceanography* 32: 1112–1123.

L'Helguen, S., C. Madec, and P.L. Corre. 1996. Nitrogen uptake in the permanently well-mixed temperature coastal waters. *Estuarine, Coastal and Shelf Science* 42: 803–818.

L'Helguen, S., J.F. Maguer, and J. Caradec. 2008. Inhibition kinetics of nitrate uptake by ammonium in size-fractionated oceanic phytoplankton communities: Implications for new production and *f*-ratio estimates. *Journal of Plankton Research* 30: 1179–1188.

Lee, J.H.W., P.J. Harrison, C. Kuang, and K.D. Yin. 2006. Eutrophication dynamics in Hong Kong coastal waters: Physical and biological interactions. In *The environment in Asia Pacific harbours*, ed. E. Wolanski, 187–206. Netherlands: Springer.

Lipschultz, F. 1995. Nitrogen-specific uptake rates of marine phytoplankton isolated from natural populations of particles by flow cytometry. *Marine Ecology Progress Series* 123: 245–258.

Lomas, M.W., and P.M. Glibert. 1999a. Temperature regulation of nitrate uptake: A novel hypotheses about nitrate uptake and reduction in cool-water diatoms. *Limnology and Oceanography* 44: 556–572.

Lomas, M.W., and P.M. Glibert. 1999b. Interactions between NH_4^+ and NO_3^- uptake and assimilation: Comparison of diatoms and dinoflagellates at several growth temperatures. *Marine Biology* 133: 541–551.

Lomas, M.W., and P.M. Glibert. 2000. Comparisons of nitrate uptake, storage and reduction in marine diatoms and flagellates. *Journal of Phycology* 36: 903–913.

Lund, B.A. 1987. Mutual interference of ammonium, nitrate and urea on uptake of ^{15}N sources by the marine *Skeletonema costatum* (Grev.) Cleve. *Journal of Experimental Marine Biology and Ecology* 113: 167–180.

McCarthy, J.J., and J.L. Nevins. 1986. Sources of nitrogen for primary production in warm-core rings 79-D and 81-E. *Limnology and Oceanography* 31: 690–700.

McCarthy, J.J., W.R. Taylor, and J.L. Taft. 1977. Nitrogenous nutrition of the plankton in the Chesapeake Bay. 1. Nutrient availability and phytoplankton preferences. *Limnology and Oceanography* 22: 996–1011.

Middelburg, J.J., and J. Nieuwenhuize. 2000. Nitrogen uptake by heterotrophic bacteria and phytoplankton in the nitrate-rich Thames estuary. *Marine Ecology Progress Series* 203: 13–21.

Parsons, T.R., K. Stephens, and T.T. Strickland. 1961. On the chemical composition of eleven species of marine phytoplankton. *Journal of Fishery Research Board of Canada* 18: 1001–1116.

Parsons, T.R., Y. Maita, and C.M. Lalli. 1984. *A manual for chemical and biological methods for seawater analysis*. New York: Pergamon.

Price, N.M., and P.J. Harrison. 1987. A comparison of methods for the measurement of dissolved urea concentration in seawater. *Marine Biology* 92: 307–319.

Redfield, A.C. 1958. The biological control of chemical factors in the environment. *American Science* 46: 205–211.

Seitzinger, S.P., C. Kroeze, A.F. Bouwman, N. Caraco, F. Dentener, and R.V. Styles. 2002. Global patterns of dissolved inorganic and particulate nitrogen inputs to coastal systems: Recent conditions and future projections. *Estuaries* 25: 640–655.

Seitzinger, S.P., J.A. Harrison, E. Dumont, A.H.W. Beusen, and A.F. Bouwman. 2005. Sources and delivery of carbon, nitrogen and phosphorous to the coastal zone: An overview of global nutrient export from watersheds (NEWS) models and their application. *Global Biogeochemistry Cycles* 19: GB4S09.

Smayda, T.J. 1990. Novel and nuisance phytoplankton blooms in the sea: Evidence for a global epidemic. In *Toxic marine phytoplankton*, ed. E. Granéli, B. Sundstrom, L. Edler, and D.M. Anderson, 29–40. New York: Elsevier.

Smayda, T.J. 1997. Harmful algal blooms: Their ecophysiology and general relevance to phytoplankton blooms in the sea. *Limnology and Oceanography* 42: 1137–1153.

Solomon, C.M., J.L. Collier, G.M. Berg, and P.M. Glibert. 2010. Role of urea in microbes in aquatic systems: A biochemical and molecular review. *Aquatic Microbial Ecology* 59: 67–88.

Suksomjit, M., K. Ichimi, K.I. Hamada, M. Yamada, K. Tada, and P.J. Harrison. 2009. Ammonium accelerates the growth rate of *Skeletonema* spp. in the phytoplankton assemblage in a heavily eutrophic embayment, Dokai Bay, Japan. *La mer* 47: 89–101.

Twomey, J.L., M.F. Piehler, and H.W. Paerl. 2005. Phytoplankton uptake of ammonium, nitrate and urea in the Neuse River estuary, NC, USA. *Hydrobiologia* 533: 123–134.

Van Mooey, B.A.S., H.F. Fredricks, B.E. Pedler, S.T. Dyhrman, D.M. Karl, M. Koblizek, M.W. Lomas, T.J. Mincer, L.R. Moore, T. Moutin, M.S. Rapper, and E.A. Webb. 2009. Phytoplankton in the ocean use non-phosphorus lipids in response to phosphorus scarcity. *Nature*. doi:10.1038/nature07659.

Wassmann, P. 2004. Cultural eutrophication: Perspectives and prospects. In *Drainage basin inputs and eutrophication: An integrated approach*, eds. P. Wassmann and K. Olli K, 224–234. Norway: University of Tromso. http://www.ut.ee/~olli/eutr/.

Wienke, S.M., and J.E. Cloern. 1987. The phytoplankton component of seston in San Francisco Bay. *Netherland Journal of Sea Research* 21: 25–33.

Wood, G.J., and K.J. Flynn. 1995. Growth of *Heterosigma carterae* (Raphidophceae) on nitrate and ammonium at three photon flux densities: Evidence for N stress in nitrate-growing cells. *Journal of Phycology* 31: 859–867.

Xu, J. 2007. Nutrient limitation in the Pearl River estuary, Hong Kong waters and adjacent South China Sea waters. Ph.D. Thesis. The Hong Kong University of Science and Technology, Hong Kong, China.

Xu, J., A.Y.T. Ho, K. Yin, X.C. Yuan, D.M. Anderson, J.H.W. Lee, and P.J. Harrison. 2008. Temporal and spatial variations in nutrient stoichiometry and regulation of phytoplankton biomass in Hong Kong waters: Influence of the Pearl River outflow and sewage inputs. *Marine Pollution Bulletin* 57: 335–348.

Xu, J., K. Yin, A.Y.T. Ho, J.H.W. Lee, D.M. Anderson, and P.J. Harrison. 2009. Nutrient limitation in Hong Kong waters inferred from comparison of nutrient ratio, bioassays and ^{33}P turnover times. *Marine Ecology Progress Series* 388: 81–97.

Xu, J., K. Yin, H. Liu, J.H.W. Lee, D.M. Anderson, A.Y.T. Ho, and P. J. Harrison. 2010. A comparison of eutrophication impacts in two harbours in Hong Kong with different hydrodynamics. *Journal of Marine Systems* 83: 276–286.

Yin, K., P.Y. Qian, J.C. Chen, D.P.H. Hsieh, and P.J. Harrison. 2000. Dynamics of nutrients and phytoplankton biomass in the Pearl River estuary and adjacent waters of Hong Kong during summer: Preliminary evidence for phosphorus and silicon limitation. *Marine Progress Ecology Series* 194: 295–305.

Yin, K., P.Y. Qian, M.C.S. Wu, J.C. Chen, L.M. Huang, X.Y. Song, and W.J. Jian. 2001. Shift from P to N limitation of phytoplankton biomass across the Pearl River estuarine plume during summer. *Marine Ecology Progress Series* 221: 17–28.

Yuan, X.C., K.D. Yin, P.J. Harrison, W.J. Cai, L. He, and J. Xu. 2010. Bacterial production and respiration in subtropical Hong Kong waters: Influence of the Pearl River discharge and sewage impacts. *Aquactic Microbial Ecology* 58: 167–179.

Yuan, X.C., P.M. Glibert, J. Xu, H, Liu, M, Chen, H.B. Liu, K. Yin, and P.J. Harrison. 2011. Inorganic and organic nitrogen uptake by phytoplankton and bacteria in Hong Kong waters. *Estuaries and Coasts*. doi:10.1007/s12237-011-9433-3.